A Star Map Recognition Algorithm Based on New Feature Extraction Method

Summary

The star sensor is the core component of the autonomous attitude measurement of the navigation body of the space vehicle. Through observing the stars in space, it calculates with several stellar vectors in order to gain high precision attitude measurement. It has various advantages and broad application prospects in space flight.

We develop a model not only exhibits the location of D-Point(the definition of D-Point would be discussed in section 2.1), but also optimize the method of star feature extraction for star tracker. Specifically, we accomplished the following:

- **Initial Coordinate Determination:** We set up an auxiliary rectangular system to model the position of intersection of optical axis and celestial sphere. Furthermore, we extended the model by reducing its parameters, achieving a more efficient way to measure the location of the intersection, that is, by knowing three sets of navigation star celestial coordinates.
- **Navigation Star Selection and Error Discussion:** We set series methods to select three finest stars from the provided data to determine D-Point by the rules stated as follows:

  1 The magnitude should be adequately large.

  2 Under the condition of satisfying the previous rule, the magnitude should be small enough.

  Besides, we have evaluated the corresponding error of the method by calculating the distance of theoretical coordinates and actual coordinates.
- **Construction of Feature Extraction Model and Implementation:** By analyzing the possible influence of recognizing D-Point, we proposed a feature extraction model. Firstly, we pre-divided the celestial sphere into several sub-blocks in order to speed up the navigation star scanning process. Then we perform match identification by giving each condition a state identifier in case to reduce the iterations of searching matching triangles to secure the position the D-Point. Lastly, the identification is being validated to ensure the accuracy of the results.

Keywords: Coordinate Systems; Selection Algorithm; Navigation Star; Feature Extraction

Contents

1 Introduction 2
1.1 Overview 2
1.2 Nomenclature 3
1.3 Simplifying Assumptions 3
2 Model Theory 4
2.1 Model of Determining the Coordinates of D-Point 4
2.2 The Navigation Star Selection Criteria and its Error Analysis 6
2.3 Feature Extraction Model 13
2.3.1 The Sub-Block Division Method 13
2.3.2 Generation and Storage of the Star Pairs 16
2.3.3 Match Identification 17
2.3.4 Validation Identification 18
3 Implementation of the Feature Extraction Model 18
3.1 Sub-Block Division 18
3.2 Star Pair Generation and Match Identification 19
3.3 Validation Identification 20
4 Strengths and Limitations 22
4.1 Strengths 22
4.2 Limitations 22
Appendices 25
Appendix A Background Knowledge 25
A.1 Basic Definition of Star Map 25
A.2 Frequently Used Coordinates in Star Map Recognition 26
A.3 The Selection of Star Catalog 27
Appendix B Calculation Results 28
B.1 The Twelve Results of The Navigation Star Selection Algorithm and Validation 28

1 Introduction

1.1 Overview

With the development of the aerospace industry, the demands for precise space vehicle control and navigation keep thriving. Projects like high-resolution earth observation and deep space exploration need extremely accurate attitudes to accomplish the tasks.[1–3] Star trackers are attitude sensors which widely applied in space vehicles, especially in satellites in advantages of high accuracy, non-drift feature, and autonomy.[4–6] The centroid locations of the observed stars are transformed into observed star vectors with model parameters[7] and then utilized by star trackers, which push forward a immense influence on precise space vehicle control and navigation.

One of the key factors that affect the performance of star trackers is the accuracy of feature extraction. High certainty of feature extraction could improve the cruise of the spacecraft and reduce unnecessary cost. In this thesis, we will start from the simplest situation to model several coordinate systems of star map for the foundation of star tracker and based on these systems to further discuss the extraction of the star feature and ultimately, to build a more accurate positioning recognition algorithm.

1.2 Nomenclature

Symbols	Description
f	The distance between the optical center and photosensitive surface (OO')
$(\alpha_i, \delta_i), i = 1, 2, 3$	The celestial coordinates, as right ascension and declination of navigation stars
$(x_i, y_i, z_i), i = 1, 2, 3$	The rectangular coordinates of navigation stars
(α_D, δ_D)	The celestial coordinates, as right ascension and declination of D-Point
$a_i, i = 1, 2, 3$	The distance between the photosensitive plane center and the centroid projection of the star ($O^{'}Q_i$)
$r_i, i = 1, 2, 3$	The distance between the optical center and the centroid projection of the star (OQ_i)
$\varepsilon_i, i = 1, 2, 3, ...C_{14}^{3}$	The error of each row of data selection
ε	The error of each scenario of data selection
N	The side length of each sub-block
$d_{m,12}, d_{m,23}, d_{m,13}$	The observation sides (angular distance) of the original triangle in match identification process
$C(d_{m,12}), C(d_{m,23}), C(d_{m,13})$	Groups of $d_{m,12}, d_{m,23}$ and $d_{m,13}$ which satisfy the matching pairs of stars
$n(d_{m,12}), n(d_{m,23}, n(d_{m,13})$	The containing star pairs of each side of match identification triangles

1.3 Simplifying Assumptions

The accuracy of our models rely on certain key, simplifying assumptions. These assumptions are listed below:

For astronomical navigation,

- the star sensor of the spacecraft would utilize nearby stars for positioning.
- the magnitude judgment threshold of the star sensor is 5.0. That is, the star sensor would tend to select the navigation stars whose magnitude is less than 5.0.

For simplifying calculation, regarding to Appendix A.1,

- while analyzing the relative position of *nearby* stars, we would assumed they are at the same plane.
- we recognize stars as stationary point light sources, located at infinity and do not affect each other.

Considering current star sensor market[13],

- while transferring pixel units to millimeters, we assumed the pixel geometry of star sensor is 512 × 512 and the image resolution is 96 dpi.

2 Model Theory

2.1 Model of Determining the Coordinates of D-Point

During the navigation process, it is vital to determine the boundary of space flight. Accordingly, we define D-Point as the intersection of optical axis and celestial sphere. Under the condition of knowing the coordinates of 3 *nearby* navigation stars P_1, P_2, P_3, whose associated coordinates are $(\alpha_i, \delta_i), i = 1, 2, 3$ in celestial coordinate system, we developed the model of determining the position of D-Point as follows.

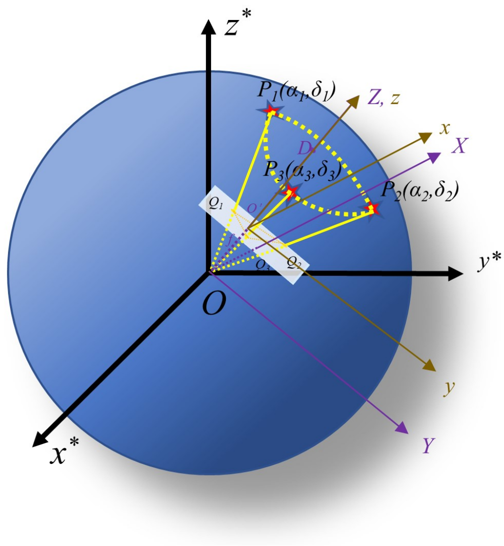

Figure 1: Model of solving D-Point, black objects serve as auxiliary spatial rectangular coordinate system, purple items function as star sensor coordinate system, and the brown lines operate as image coordinate system

As Figure 1 illustrates, we set an auxiliary rectangular coordinate system $O - x^*y^*z^*$. Initially, the distance of OO' is f and the celestial coordinates of P_1, P_2, P_3 are $(\alpha_i, \delta_i), i = 1, 2, 3$. Under the rule of projection, the celestial coordinates for Q_1, Q_2, Q_3 are the same as former. Therefore, the rectangular coordinates for Q_1, Q_2, Q_3 can be acquired by following formulas:

$$r_i = \sqrt{f^2 + a_i^2} \tag{1}$$

$$(x_i, y_i, z_i) = \begin{cases} x_i = r_i \cos\delta_i \cos\alpha_i \\ y_i = r_i \cos\delta_i \sin\alpha_i \quad i = 1, 2, 3 \\ z_i = r_i \sin\delta_i \end{cases} \tag{2}$$

Thus the normal vector of photosensitive plane, also the vector of *z-axis of the star sensor coordinate system*, can be attained by

$$\vec{n} = \overrightarrow{Q_1Q_2} \times \overrightarrow{Q_1Q_3} = \begin{vmatrix} \vec{i} & \vec{j} & \vec{k} \\ x_2 - x_1 & y_2 - y_1 & z_2 - z_1 \\ x_3 - x_1 & y_3 - y_1 & z_3 - z_1 \end{vmatrix} = a\vec{i} + b\vec{j} + c\vec{k} = (a, b, c) \tag{3}$$

where $a = (y_2 - y_1)(z_3 - z_1) - (y_3 - y_1)(z_2 - z_1)$, $b = (z_2 - z_1)(x_3 - x_1) - (z_3 - z_1)(x_2 - x_1)$, $c = (x_2 - x_1)(y_3 - y_1) - (x_3 - x_1)(y_2 - y_1)$. In this situation, the celestial coordinate *value* of D-Point is

$$\alpha = \arctan\frac{b}{a} \tag{4}$$

$$\delta = \arctan\frac{c}{f} \tag{5}$$

Based on the assumptions in 1.3. If the star sensor choose the navigation stars near the spacecraft, the rough direction of the normal vector of photosensitive plane should be in the range of three navigation stars. So the signs of α_D, α_i should be consistent with $(\alpha_i, \delta_i), i = 1, 2, 3$. Specifically, as Figure 1 shows, let the navigation stars in the first octant. In this degree, the signs of α_D, δ_D would be positive.

Having discussed how to Determine the D-Point Coordinates, the remaining of this subsection addresses ways of extending the existed model. Based on reality, measuring the f-distance would raise additional cost for related administrative units [9], this subsection would model D-Point Coordinates without using parameter f.

From 1.3, we represent the radius of celestial sphere as R. Intuitively, $R \to +\infty$. Thus from the perspective perpendicular to the photosensitive plane, we can depict the diagram as Figure 2.

Under the law of projection, we could readily judge that $\triangle P_1P_2P_3$ is similar to $\triangle Q_1Q_2Q_3$. In consonance with previous experience,

$$(x_i, y_i, z_i) = \begin{cases} x_i = R \cos\delta_i \cos\alpha_i \\ y_i = R \cos\delta_i \sin\alpha_i \quad i = 1, 2, 3 \\ z_i = R \sin\delta_i \end{cases} \tag{6}$$

Again, the normal vector of photosensitive plane can be attained by

$$\vec{n} = \overrightarrow{Q_1Q_2} \times \overrightarrow{Q_1Q_3} = \begin{vmatrix} \vec{i} & \vec{j} & \vec{k} \\ x_2 - x_1 & y_2 - y_1 & z_2 - z_1 \\ x_3 - x_1 & y_3 - y_1 & z_3 - z_1 \end{vmatrix} = a\vec{i} + b\vec{j} + c\vec{k} = (a, b, c) \tag{7}$$

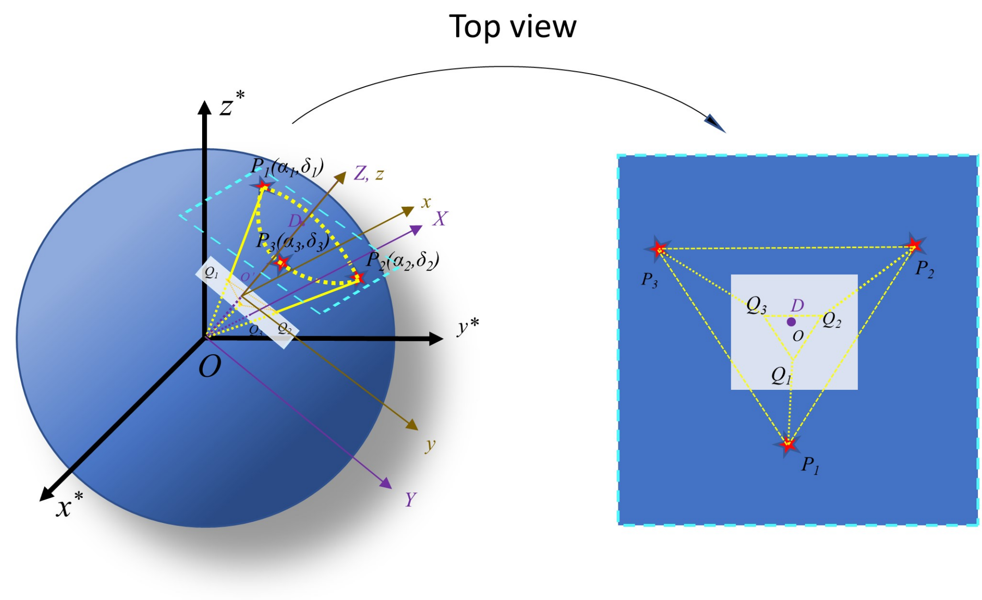

Figure 2: Top view of star sensor

where $a = (y_2 - y_1)(z_3 - z_1) - (y_3 - y_1)(z_2 - z_1)$, $b = (z_2 - z_1)(x_3 - x_1) - (z_3 - z_1)(x_2 - x_1)$, $c = (x_2 - x_1)(y_3 - y_1) - (x_3 - x_1)(y_2 - y_1)$. In this situation, the celestial coordinate *value* of D-Point is

$$\alpha = \arctan \frac{b}{a} \tag{8}$$

$$\delta = \arctan \frac{c}{\sqrt{a^2 + b^2 + c^2}} \tag{9}$$

Note that parameter R is removed by the process of dividing. Similarly, The sign of these values should be consistent with the navigation stars based on simplifying assumptions.

2.2 The Navigation Star Selection Criteria and its Error Analysis

Despite we have constructed the model in the previous subsection, generally speaking, as the actual scenario shows, there are more than three stars in the field of view of the star sensor. Hence a selection of proper navigation stars must be applied. Through our research, a good selection algorithm ought to obey the following rules stated in A.3.

Reference [12] has discussed the accepted Field of View (FOV) of star sensor. Finally, we use $\theta = 8°$ as FOV of star sensor, which is consistent with the literature. The following table exhibits part of the data implemented in reference [15].

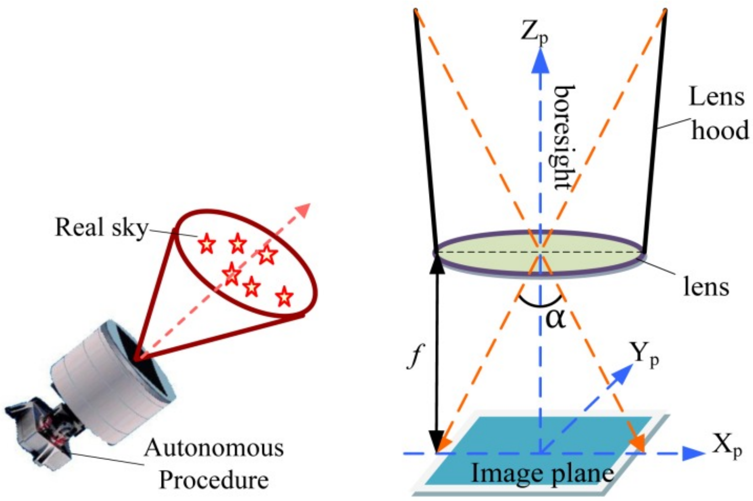

Figure 3: The mechanism of star sensor identification, note that the photosensitive plane is not plotted in the diagram

FOV/°	Focal Length/mm	SZA = 20°	SZA = 40°	SZA = 60°	SZA = 80°
Ø 4	180	12.93%	28.2%	58.7%	85.4%
Ø 6	121	9.2%	25.6%	61%	85.6%
Ø 8	92	6.25%	22.3%	62.6%	86.4%
Ø 10	73	3.6%	16.6%	56.4%	86.18%
Ø 12	61	1.89%	11.1%	50.7%	84.5%

Figure 4: Part of the data in parameter optimization in reference[15], SZA represents Sun Zenith Angle, the percentage stands for the detection rate for each condition.

Suppose the visual axis of the star sensor points to the right ascension, the declination is (α_0, δ_0), and the radius of circular FOV is R. When the whole celestial sphere is photographed, the right ascension α and the declination δ of the observation stars which satisfy the following two conditions simultaneously, the star can be successfully imaged in the optical system of the star sensor:

- $$\alpha \in \left(\alpha_0 - \frac{R}{\cos\delta_0}, \alpha_0 + \frac{R}{\cos\delta_0}\right) \tag{10}$$
- $$\delta \in (\delta_0 - R, \delta_0 + R) \tag{11}$$

Ideally, assume that M navigation stars are evenly distributed in the celestial sphere. For a circle with a radius of θ, the average number of navigation stars that appear in FOV is:

$$N = \frac{M(1-\cos\theta)}{2} \tag{12}$$

For a $\theta \times \theta$ square FOV, the average number of navigation stars that appear in FOV is:

$$N = \frac{M\left(1 - \cos\theta\right)}{\pi} \tag{13}$$

From reference [13], the squared-design FOV takes the monopoly of the current star sensor market. Therefore, by equation (13), the average number of navigation stars that appear in FOV is approximately around 15. Based on this foundation, here we implement two sets of conditions to discover the criteria of selecting proper navigation stars in order to ensure the high accuracy location of D-Point. The data we use is the simple star catalog provided in Annex 1.

Before presenting our results, we would like to address the how we process the provided data.

- **Step 1** From reference [16], we would give two basic standards of our selection:

1 we defined the maximum sensitive magnitude value of star sensor at 5.0, that is, we denote stars whose magnitude are less than 5.0 with blue dots, and red dots are representing stars whose magnitude are greater than 5.0. To be more precise, we define "bright" stars as their magnitude are less than 5.0 and vice versa.

2 we defined a parameter to measure the aggregation of the stars. That is, when the longest distance between two stars are nearer than 4.0, we call this group of stars are "dense". Otherwise, we call them "sparse" Then we plotted the whole dataset.

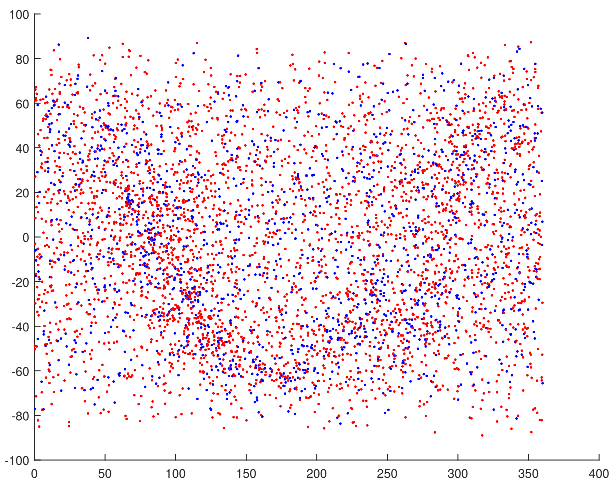

Figure 5: The initial navigation star map. The vertical axis represents the declination, and the horizontal axis represents the right ascension

- **Step 2** Under different criteria, we selected a random region from the original star map where contains 15 navigation stars and choose the navigation star which is nearest to the center of the selected region as D-Point, whose celestial coordinates are (α_0, δ_0). The remaining stars could form C_{14}^3 kinds of triangles. Each apex of corresponding triangle could be denote as $(\alpha_i, \delta_i), (\alpha_j, \delta_{ij}), (\alpha_k, \delta_k)$.

- **Step 3** By repetitive applying equations (6)-(9), we can computed the C_{14}^3 theoretical values of D-Point, whose coordinates are $(\alpha^{'}, \delta^{'})$.

- **Step 4** The error of theoretical value and actual value could be figured out by calculating their spatial distance.

$$\varepsilon_i = \sqrt{(\alpha\prime - \alpha_0)^2 + (\delta\prime - \delta_0)^2} \tag{14}$$

- **Step 5** By doing duplicate calculations and comparisons, the minimum error of each criterion should be the minimum value of ε_i

$$\varepsilon = \min \varepsilon_i \tag{15}$$

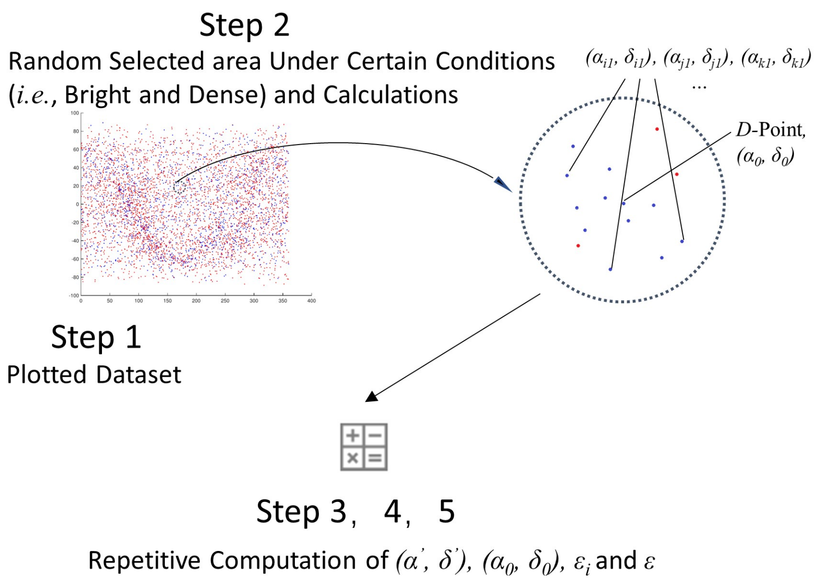

Figure 6: Our method

We perform the above algorithm under the two sets of conditions. For the magnitude of star, we divided them into Bright/Dim groups. For the aggregation of star, we divided them into Sparse/Dense groups. Each time we randomly selects two conditions for classification criteria. The raw results are shown in Appendix B.1. From them, we draw the following table:

	Bright and Sparse	Bright and Dense	Dim and Sparse	Dim and Sparse
1	5.4796	2.9914	3.4526	10.8948
2	12.0920	8.9973	13.6996	7.0012
3	12.9183	0.1180	11.5610	7.0637
avg.	10.1633	4.3557	9.5711	8.3199

Table 1: The processed result for each condition

avg.of	Bright	Dim	Sparse	Dense
	7.2595	8.8566	9.8672	6.0489

Table 2: The average result for each single condition

From what is implemented above and background knowledge in Appendix A.3, we can conclude that in the case of even star distribution: the bright error is lower than the dark group, and the dense error is lower than the sparse group. To conclude, the selection of stars must be satisfied the following statements:

1 The magnitude should be adequately large. The term "adequate" means the magnitude should be large enough to let the star to be captured by the star sensor.

2 Under the condition of satisfying the previous rule, the magnitude should be small enough. That is not only because the memory of star sensor is limited, but also would cost more time for other navigation component to do the analysis.

Thus far, this subsection has argued the navigation star selection principle. Nevertheless, it is limited to the amount of the utilization of three stars. Therefore, the remaining of this subsection would discuss whether the number of stars used for star navigation and the geometric position between the stars will affect the positioning accuracy.

Firstly, we would discuss the star amount influences. Consider current 3-star positioning model, which is modeled after the assumption that the stars are distributed evenly. However, the real situation may include region that the stars are distributed unevenly, e.g., the selected stars would present on a same line as shown below:

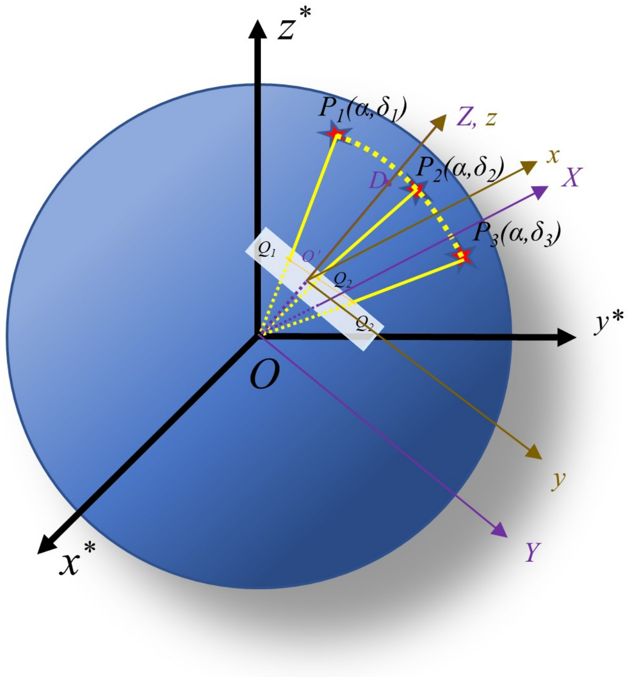

Figure 7: The failure of the model presenting in Section 2.1

According to figure 7, P_1, P_2, P_3 are accidentally selected as navigation stars. In this situation, the projection of the stars would be a line. Therefore, the normal vector of photosensitive plane does not exist. Hence the model would fail.

To solve this problem, based on the algorithm stated in Section 2.2, when the method fails. Another measure must be applied. From the three selected stars, the star sensor processing unit should choose two brightest stars, then separately taking them as two centers of two independent circles. The radius of these circles gradually growing from zero until them intersect with another navigation star or the boundary of FOV.

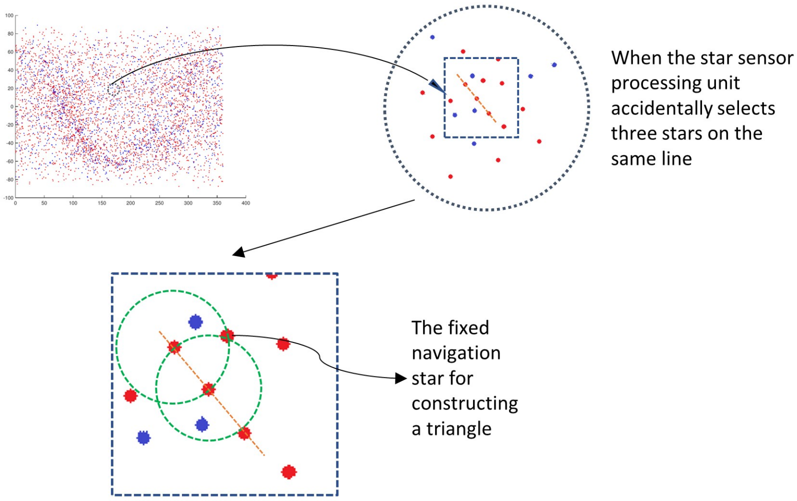

Figure 8: The schematic diagram for solution

As for the amount of the navigation stars used for positioning, reference [14] defines how an observation mode matches a navigation pattern.

1 The measured angular distance of each observation star *pair* matches the corresponding navigation star diagonal distance within the angular distance decision threshold of star sensor;

2 The magnitude of each observation star and the corresponding navigation star matches within the magnitude judgment threshold range of star sensor.

The sum of *the number of* magnitude and *the number of* angular distances is called the feature dimension of this navigation pattern. Obviously, a star map pattern consisting of n stars has a characteristic dimension that

$$V = C_n^2 + n \tag{16}$$

Reference [17] has made statistics on the relationship between the feature dimension of the star map model and the ambiguity matching rate. The result shows that the ambiguity matching rate decreases with the increase of the feature dimension of the star map. It can be seen that increasing the number of navigation stars constituting the star map can bring significant improvement to the accuracy of the algorithm recognition rate.

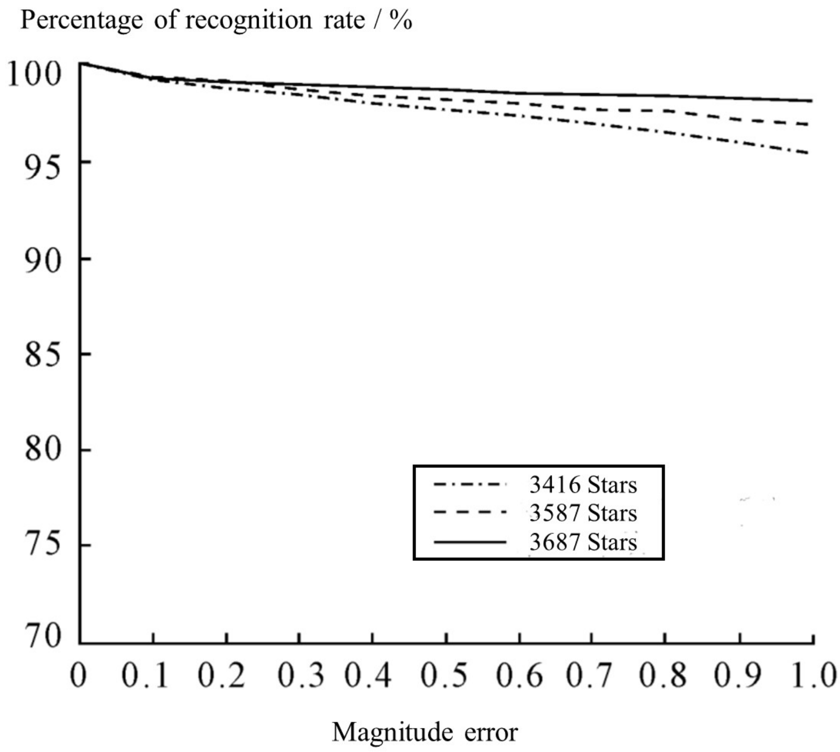

Figure 9: The result between n and recognition rate

Based on what is discussed above, we can clearly see that the geometry distribution and the number of navigation stars have a great impact on recognizing D-Point. Thus they have an immense influence on the positioning.

2.3 Feature Extraction Model

Actually, the triangle algorithm proposed previously is a mature star map recognition method. If the coordinates of a navigation triangle matches the observation triangle, the recognition is successful. The flooding number of navigation triangles is the most crucial problem faced by the algorithm. The existence of this problem makes the algorithm recognize rate relatively low. On the other hand, the required storage for these triangles is relatively large, and it would be a time-consuming process. This subsection aims to develop a feature extraction pre-processing process in order to reduce the amount of the triangles and increase the efficiency of recognition.

2.3.1 The Sub-Block Division Method

Normally, the arrangement of the navigation stars in the navigation catalog is irregular, which means that if a navigation star of a certain range of celestial regions pointed by a certain visual axis is to be selected, the entire navigation star catalog must be traversed entirely. Obviously, the efficiency of such a search is very unsatisfied. Therefore, the celestial sphere is often divided into several sub-blocks to form the division of the star catalog.

The general procedure of our sub-block division can be performed as follows:

- **Step 1** The celestial sphere is evenly divided into six regions by the inscribed cube of the celestial sphere, The line between the center of the celestial sphere and the four vertices on each side of the cube forms a cone, the cone and the sphere intersect and divide it into six pieces: $S_1 \sim S_6$
- **Step 2** For each region in $S_1 \sim S_6$, we divide it into small blocks of $N \times N$. Thus, the entire celestial sphere can be divided by $6 \times (N \times N)$ sub-blocks. Divided in this way, the area contained in each sub-block is equal and corresponds to a range in which FOV is $\left(\frac{90^\circ}{N}\right) \times \left(\frac{90^\circ}{N}\right)$.

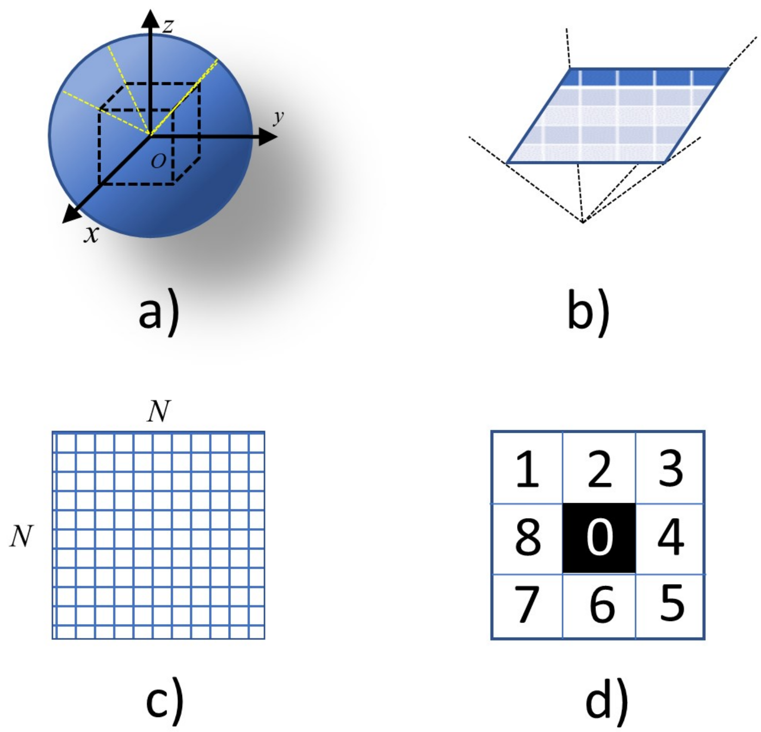

Figure 10: The sub-block division process

According to the above method to divide the celestial sphere, scan the navigation star catalog so that each navigation star is attributed to the corresponding sub-block, and a partition table is established. The form of the partition table is as shown in figure 11.

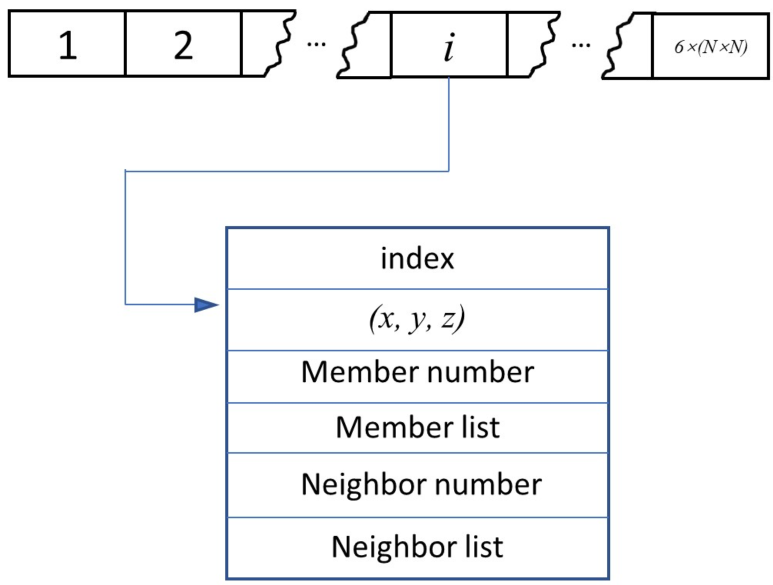

Figure 11: Partition table structure

Each partition records the following information:

- Index—the sequence number of the sub-block;
- (x, y, z)—the directional vector of each partition;
- Member number—the total number of the stars contained in current sub-block;
- Member list—the list of the stars of current sub-blocks;
- Neighbor number—the adjacent sub-block number of current sub-block;
- Neighbor list—the list of neighboring blocks of current sub-block;

Note that (x, y, z) are sorted in ascending (or descending) order. If the direction vector of the visual axis is known (by the discussed method of Section 2.1-2.2), the corresponding sub-block and the adjacent sub-block can be quickly found in certain celestial area. In order to efficiently retrieve the navigation star of the adjacent area from the serial number of the navigation star, the serial number of the sub-block to which the navigation star belongs is also stored in the navigation star catalog.

2.3.2 Generation and Storage of the Star Pairs

Direct storage of all navigation triangles will result in large storage capacity and redundant matching. With this in mind, triangle matching is implemented here in the form of storing star diagonals. Since the number of pairs of stars is much smaller than the number of triangles, the storage capacity will be greatly reduced. At the same time, a reasonable storage star pair can facilitate quick retrieval and speed up the recognition.

The generation process of the star pairs is as follows: scan the filtered navigation star catalog. If there are 2 stars whose angular distance is less than d, record the angular distance and the serial number of 2 stars (star pairs). Here, d is the diagonal of FOV.

we proposed the pairs of stars are stored in ascending order of angular distance. In order to facilitate the matching search of the star diagonal distance, all the angular distances are divided into a plurality of interval segments, and each interval segment represents an angular interval of 0.01°. In this way, calculating the angular distance of the two observation stars will quickly find a pair of navigation stars that may match them.

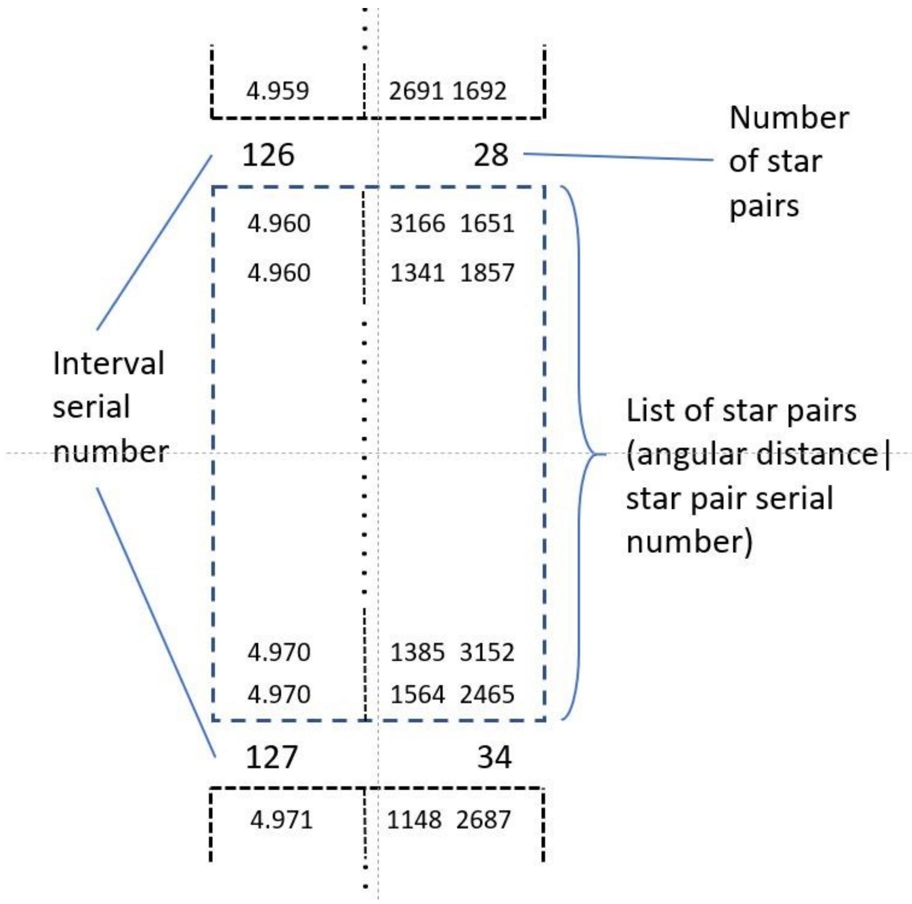

Figure 12: Structure chart of star pair storage. Here is an datasheet example of interval serial number 126

2.3.3 Match Identification

Let $d_{m,12}, d_{m,23}$ and $d_{m,13}$ to be the observation sides (angular distance) of the original triangle, the match identification process is to find the matching pairs in the star pair database according to the 3 angular distances. Let the groups of $d_{m,12}, d_{m,23}$ and $d_{m,13}$ which satisfy the matching pairs of stars call $C(d_{m,12}), C(d_{m,23})$ and $C(d_{m,13})$. The containing star pairs is $n(d_{m,12}), n(d_{m,23})$ and $n(d_{m,13})$. The process of triangle matching is actually looking for 3 pairs of stars $P_1 \in C(d_{m,12}), P_2 \in C(d_{m,23}), P_3 \in C(d_{m,13})$ and fulfills the condition that P_1, P_2 and P_3 end to end. That is, there is only one common star between the two. (P_1, P_2, P_3) which satisfies such condition can constitute a matching triangle of the observation triangle.

As an optimization of conventional match method[15], we put forward the successive operation to speed up the matching time:

1 **Scan** $C(d_{m,12})$, set the state of the group of the navigation star contained in all star pairs to I, and record the serial number j of the other star that forms the star pair;

2 **Scan** $C(d_{m,23})$, if the state of the navigation star contained in the star pair has been set to condition I, set the condition of this navigation star to II, and note the serial number k of another navigation star that forms the star pair;

3 **Scan** $C(d_{m,13})$, if $(j, k) \in C(d_{m,13})$, then a matching triangle is found, and the state of another navigation star that forms a star pair with (j, k) is changed from II to III. (i, j, k) is the navigation triangle that matches the observed triangle.

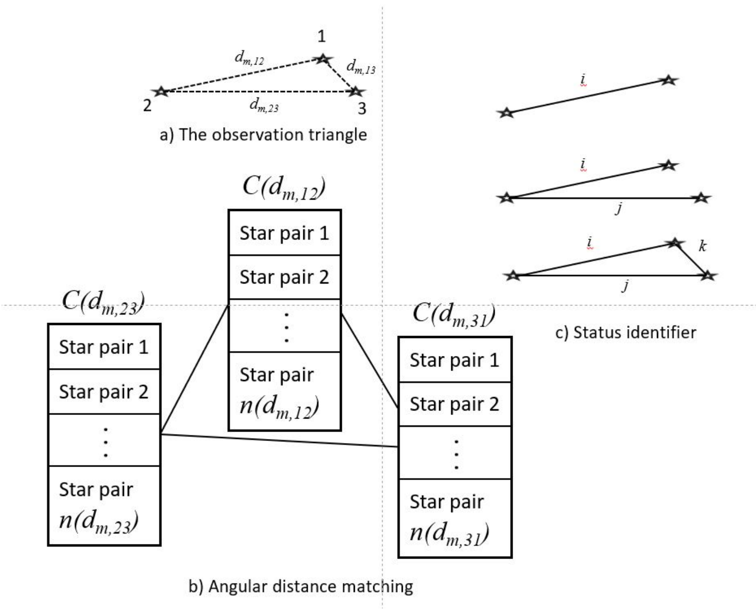

Figure 13: Matching identification process

2.3.4 Validation Identification

Through the above identification process, the navigation triangles which the observation triangle can match may not be unique. At this time, other methods must be relied on for further filtering.

The basic idea of verifying identification is: If the recognition is correct, i.e., the navigation triangle is the correct match of the observed triangles, the pose calculated using these matches should be accurate. Furthermore, a simulated star map (called a reference star map) generated according to this attitude should also be consistent with the original observation star map.

3 Implementation of the Feature Extraction Model

From what is discussed above, we implemented our model into practice. In this subsection, we would use four star maps given in Annex 2 to determine the star number corresponding to each star image.

3.1 Sub-Block Division

From the proposed model and reference[13], we supposed the FOV of the Current prevailing star sensor is fixed at $12° \times 12°$. As Section 2.3.1 stated, in order to make full use of FOV of star sensor, we set parameter $N = 9$, which lets the visible range of navigation stars falls in $10° \times 10°$. So the number of sub-blocks should be $6 \times (9 \times 9) = 486$ pieces.

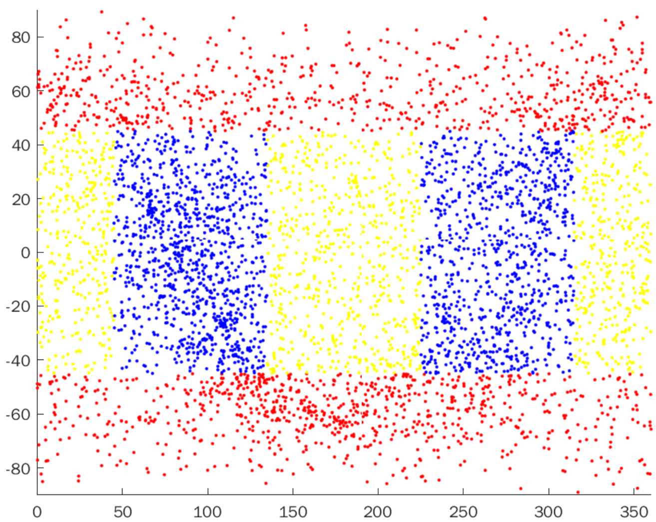

Figure 14: An example of sub-block division, different sub-blocks are marked as different colors, $N = 1$

3.2 Star Pair Generation and Match Identification

Based on Section 2.3.2, we obtained C_{4098}^2 star pairs. Due to space limit, we present part of the complete list of star pairs generated by Annex 1 below.

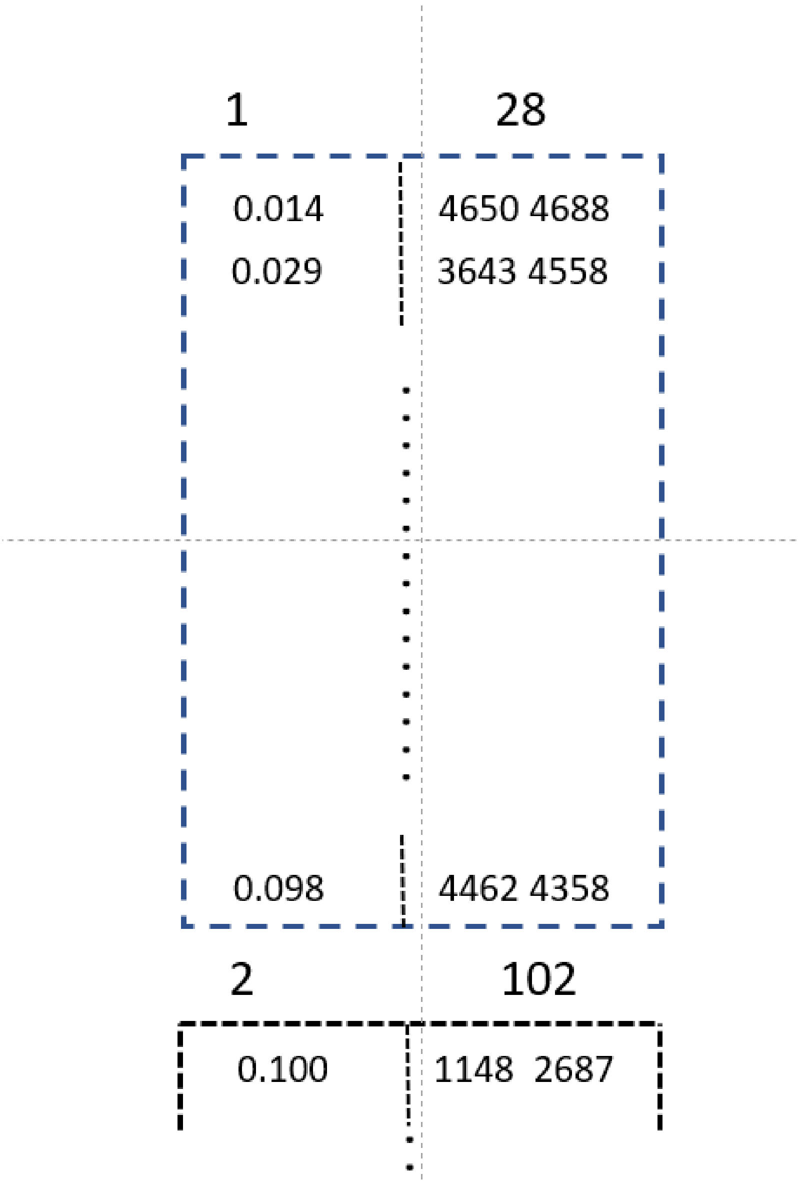

Figure 15: part of the complete list of star pairs generated by Annex 1

As for Match Identification, in general, the traversal method for triangle matching search requires $n(d_{m,12}) \times n(d_{m,23}) \times n(d_{m,13})$ times of comparison operations, if each edge corresponds to the matching star If the number of pairs of stars contained in the set is about 100, then one match requires 10^6 comparison operations. Such a search takes a considerable amount of time. However, with the method of setting the status identifier stated in 2.3.3, as introducing the status identifier, the number of searches greatly reduce to $n(d_{m,12}) + n(d_{m,23}) + n(d_{m,13})$.

3.3 Validation Identification

As for the data provided in Annex 2, we performed our algorithm, and the results are illustrated as follows.

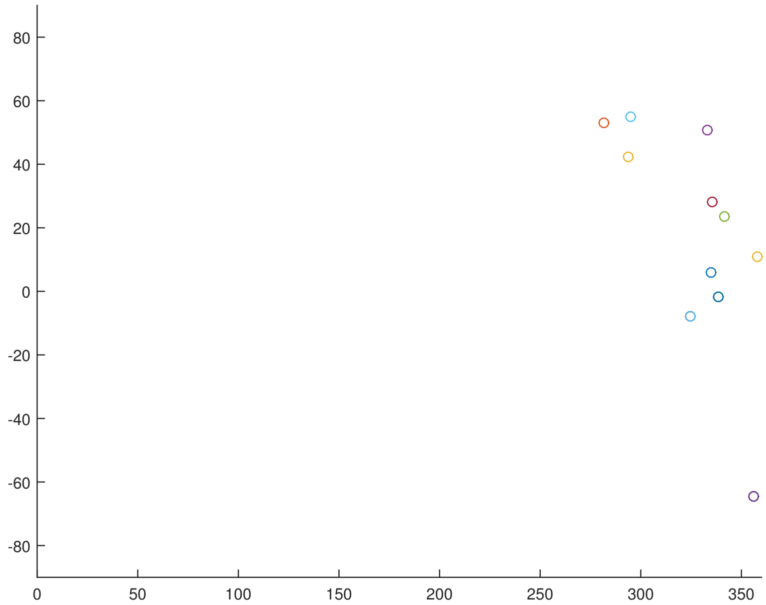

Figure 16: The result of starmap01

The corresponding serial number of the original starmap for each star is: 3804, 4650, 4046, 3472, 4688, 4061, 4462, 4867, 1774, 4892, 4867, 4650, 4462, 3804, 4650.

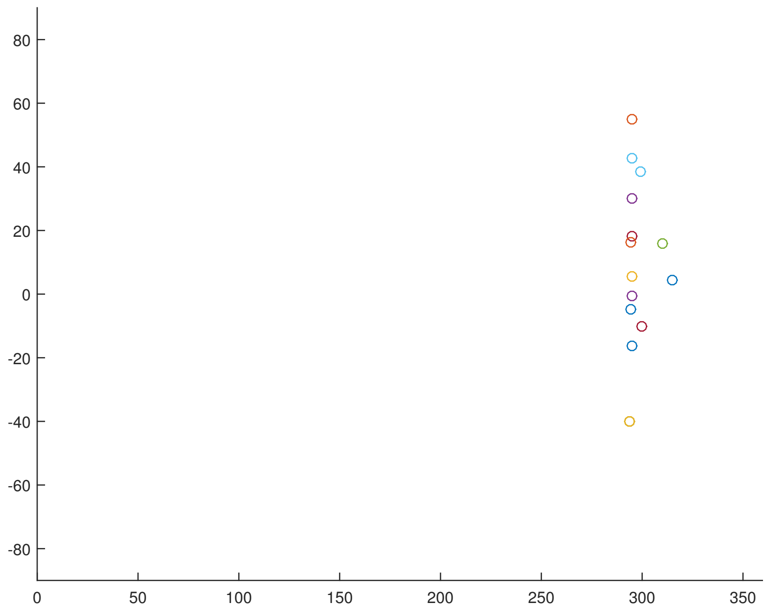

Figure 17: The result of starmap02

The corresponding serial number of the original starmap for each star is: 3760, 4061, 4046, 3784, 3643, 4462, 3074, 4523, 4229, 3643, 3804, 3074, 4523, 3740, 4546.

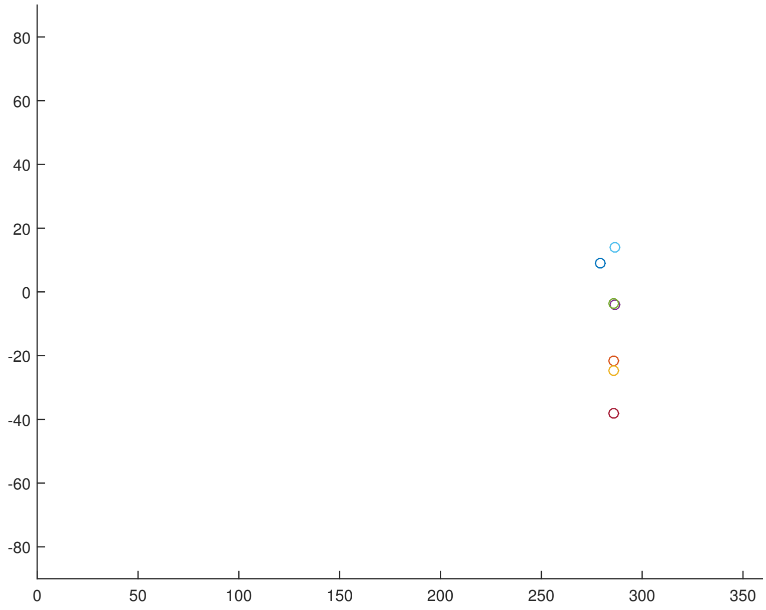

Figure 18: The result of starmap03

The corresponding serial number of the original starmap for each star is: 228, 2951, 3643, 2957, 4650, 1442, 4724.

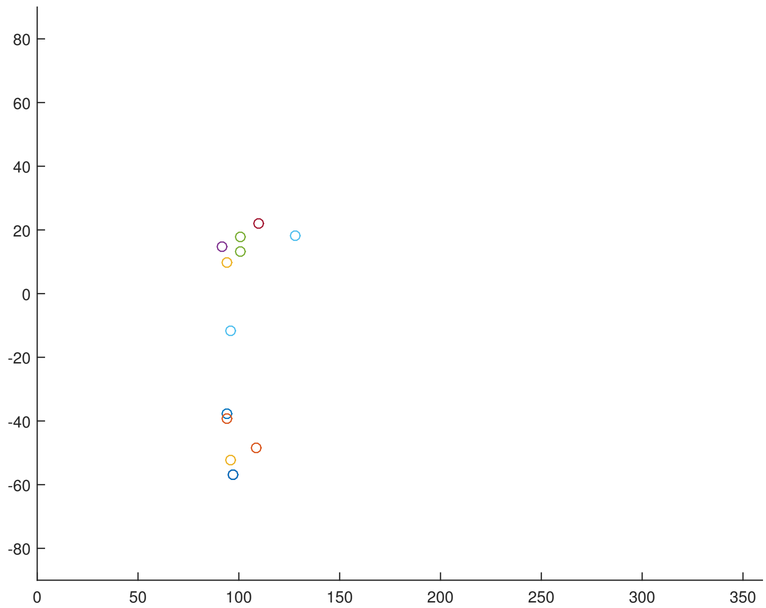

Figure 19: The result of starmap04

The corresponding serial number of the original starmap for each star is: 979, 1278, 4, 629, 4688, 1462, 4558, 4229, 4724, 1278, 4506, 3784, 4109.

4 Strengths and Limitations

4.1 Strengths

- With three sets of celestial coordinates, our model is able to produce the celestial coordinates of D-Point, which is practical in actual scenario.
- By the sub-block division prerequisite, the efficiency of our model has been improved comparing to the conventional model. Moreover, this technique does not required to do a traverse of all star map data.

4.2 Limitations

- While our model is capable of extracting accurate star features, it does not apply on circular FOV star sensors. Regarding the monopoly of the current market and time limit, we did not model this situation.
- In real scenario, the implement of navigation star selection, feature extraction are undergo through a spherical plane. Our model consider it to be a flat plane in order to obtain a simplified calculation.

References

[1] Schmidt, U., Elstner, C., & Michel, K. (2008). ASTRO 15 star tracker flight experience and further improvements towards the ASTRO APS star tracker. In *AIAA Guidance, Navigation and Control Conference and Exhibit* (p. 6649).

[2] Schmidt, U. (2005, August). ASTRO APS-the next generation Hi-Rel star tracker based on active pixel sensor technology. In *AIAA Guidance, Navigation, and Control Conference and Exhibit* (p. 5925).

[3] Blarre, L., Ouaknine, J., Oddos-Marcel, L., & Martinez, P. E. (2006). High accuracy Sodern star trackers: recent improvements proposed on SED36 and HYDRA star trackers. In *AIAA Guidance, Navigation, and Control Conference and Exhibit* (p. 6046).

[4] Liebe, C. C. (2002). Accuracy performance of star trackers-a tutorial. *IEEE Transactions on aerospace and electronic systems*, 38(2), 587-599.

[5] Eisenman, A. R., & Liebe, C. C. (1998, March). The advancing state-of-the-art in second generation star trackers. In *1998 IEEE Aerospace Conference Proceedings* (Cat. No. 98TH8339) (Vol. 1, pp. 111-118). *IEEE*.

[6] Steyn, W., Jacobs, M., & Oosthuizen, P. (1997, February). A high performance star sensor system for full attitude determination on a microsatellite. In *Workshop on Control of Small Spacecraft at the 1997 Annual AAS Guidance and Control Conference*, Breckenridge, CO, USA.

[7] Luo, L., Xu, L., & Zhang, H. (2015). Improved centroid extraction algorithm for autonomous star sensor. *IET Image Processing*, 9(10), 901-907.

[8] `https://en.wikipedia.org/wiki/Celestial_sphere`

[9] Wolf, P., Skultety-Betz, U., Schulte, C., Stierle, J., Haase, B., & Renz, K. (2010). *U.S. Patent No. 7,760,335*. Washington, DC: U.S. Patent and Trademark Office.

[10] `https://web.njit.edu/~gary/202/Lecture16.html`

[11] `https://en.wikipedia.org/wiki/Star_catalogue`

[12] Wang, W., Wei, X., Li, J., Du, J., & Zhang, G. (2019). Optical Parameters Optimization for All-Time Star Sensor. *Sensors*, 19(13), 2960 .

[13] Bin L., Hai, Zhu., Tao Z., & Yu, T.. (2016). Research Status and Development Trend of Star Sensor Technology. *Chinese Optics*, 9(1), 16-29 (in Chinese).

[14] Van Bezooijen, R. W. H. (1989). Autonomous star referenced attitude determination. In *Guidance and Control 1989* (pp. 31-52).

[15] Xin-guo, Z. G. J. W., & Jiang, J. (2006). Star Map Identification Based on a Modified Triangle Algorithm . *Acta Aeronautica Et Astronautica Sinica*, 6, 031.

[16] Bin L., Hai, Zhu., Tao Z., & Yu, T.. (2016). Research Status and Development Trend of Star Sensor Technology. *Chinese Optics*, 9(1), 16-29.

[17] Hong, K., Zheng Z. & Guo, Y. (2010). Establishment of Navigation Star Table in Star Sensor. *Journal of Astronautics* , 13(4), 0.

Appendices

Appendix A Background Knowledge

A.1 Basic Definition of Star Map

In order to describe the orientation of the star, a coordinate system must need to be established to represent the position information of the star at a certain moment by the coordinate value. This coordinate system is the celestial coordinate system. The astronomical definitions and concepts related to the celestial coordinate system are as follows:

- **Celestial sphere** The establish of celestial sphere is formed on the idea to fit people's intuitive feelings in astronomy. It sets the universe to be spherical, as shown in Figure 20. The celestial sphere is an imaginary sphere with an *infinite* radius , which centering the center of the earth.[8]

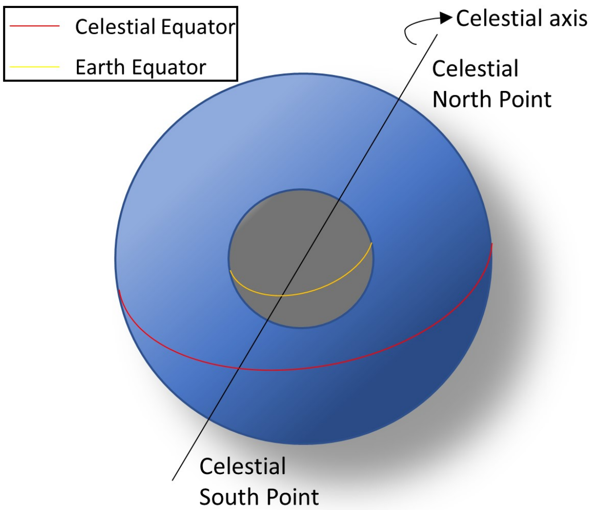

Figure 20: Celestial Sphere

- **The main elements of the celestial sphere** The main elements of the celestial sphere contains the celestial equator, the celestial plane, etc.
  - **The celestial equator and the celestial plane** The celestial equator is defined as a circumference lays on the same plane with the center of the celestial sphere and perpendicular to the celestial axis. The plane where the celestial equator is located is called the celestial plane.
  - **The ecliptic plane and the ecliptic** The average orbital plane of the earth's center orbiting the sun is called the ecliptic plane. The great circle

formed by the intersection of the ecliptic surface and the celestial sphere is called the ecliptic.

- **vernal equinox** The equator and the ecliptic intersect at two points. The point where the celestial equator is transferred from the southern hemisphere to the northern hemisphere is called the vernal equinox.

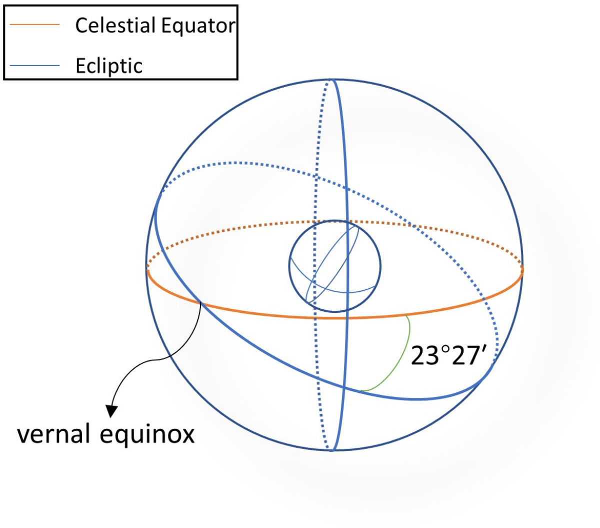

Figure 21: The main elements of the celestial sphere

Figure 21 shows the main elements discussed above.

A.2 Frequently Used Coordinates in Star Map Recognition

In the related work of star map recognition, there are three coordinates frequently used. This section would introduce their basic definition as follows:

- **Celestial coordinate system** In astronomy, a celestial coordinate system is a system for specifying positions of satellites, planets, stars, galaxies, and other celestial objects. This coordinate system takes the plane of celestial equator as the fundamental plane (plane that 0 latitude lays on). Define primary direction circle as a circle vertical to the celestial equator and passed vernal equinox. The primary direction circle determines the 0 -180 circle, orienting at vernal equinox. The celestial coordinate system uses the right ascension and declination as the coordinate quantities. The former is ranging from 0 to 360 , and the latter varies from -90 to 90 , taking the north position as the positive direction. Figure 22 depicts this system.

- **Star sensor coordinate system and image coordinate system** The star sensor coordinate system Takes the projection center as the coordinate origin, and the optical axis as the z-axis. A straight line parallel to both sides of

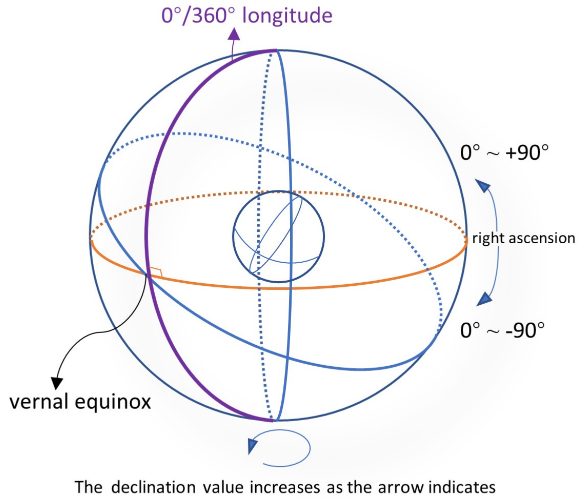

Figure 22: Celestial coordinate system

the photosensitive surface is regarded as the x-axis and the y-axis.The Image coordinate system takes the center of the photosensitive surface as the coordinate origin, and the line parallel to both sides of the photosensitive surface is the x-axis and the y-axis, Figure 23 is a schematic diagram of a star sensor coordinate system its relevant image coordinate system.

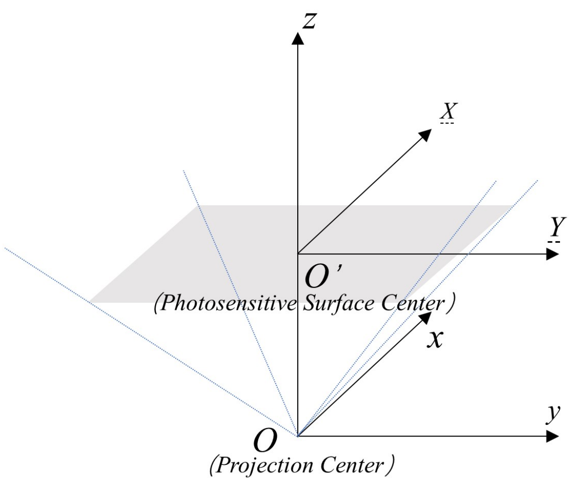

Figure 23: Star sensor coordinate system and image coordinate system

A.3 The Selection of Star Catalog

A star catalog is an astronomical catalog that lists stars. In astronomy, many stars are referred simply by catalog numbers. Star catalog and star map processing are the basic work of star map recognition. Therefore, the information of the star is indispensable. The star information utilized by the star sensor mainly includes the position of the star (right ascension, declination coordinates) and brightness. The star sensor′s memory stores basic information about a range of stars in a range of brightness. This simple star catalog is often referred to as the Guide Star Catalog (GSC) . In order to speed up the retrieval speed of navigation stars, it is usually necessary to divide the star catalog[11, 14]. The division of the star catalog plays an important role in improving the star map recognition and star tracking efficiency.

Name	RA(1950)	Dec(1950)	pm	angle	v_{rad}	Sp Type	m_V	$B-V$	$U-B$	$R-I$	π_{trig}	M_V
Sun						G2 V	-26.72	0.65	0.10			4.85
NN	00 00 06	-34 29.7	0.758	168.6		DC9	14.90	0.46	-0.44		75.2	14.28
GJ 1001	00 02 05	-40 57.8	1.618	154.5	-3	M3.5	12.84	1.63	1.30	1.23	104.2	12.93
NN	00 02 16	+34 22.8	0.776	83.0	+6.4 VAR	G2 V	6.11	0.62	0.09		29.8	4.56
NN	00 02 21	+22 59.5	0.380	91.5		G9 V	7.82	0.74	0.29	0.33		5.78
Gl 1	00 02 28	-37 36.2	6.097	112.5	22.9	M4 V	8.54	1.46	0.96	0.92	221.8	10.27
Gl 2	00 02 32	+45 30.6	0.894	100.5	0.1	dM2 e	9.93	1.49	1.18	0.85	87.0	9.63
NN	00 02 43	+48 12.0	0.009	305.5		G5	8.30					6.84
Gl 3	00 02 48	-68 06.2	0.582	190.7	41	K5 V	8.48	1.06	1.03	0.42	72.5	7.1
NN	00 02 54	-50 20.0	0.167	276.0		M5	11.95	1.50		+0.95t		10.31
Gl 4 A	00 03 02	+45 32.2	0.839	101.8	+0.0 SB	dK6 e	8.97	1.44	1.21	+0.71 J	87.0	8.67
Gl 4 B	00 03 02	+45 32.1	0.885	98.3	0.1	M0.5 V	9.02	1.45	1.20		87.0	8.72
Gl 4.1A	00 03 38	+58 09.5	0.260	76.7	-11.6	G5 V	6.43c	+0.64c	+0.11c		46.5	4.77c
Gl 4.1B	00 03 38	+58 09.5	0.260	76.7	-16	dG8	7.20c	+0.78c	+0.33c		46.5	5.54c
NN	00 03 40	-66 07.5	0.593	160.6		M4	12.16	1.55		1.04		10.86
Gl 4.2A	00 03 44	-49 21.2	0.592	93.9	2.6	G1 IV	5.71	0.52	0.03	0.17	48.3	4.13
Gl 4.2B	00 03 44	-49 21.2	0.592	93.9			11.50				48.3	9.9 *
Gl 5	00 04 01	+28 44.7	0.422	114.1	-5.5	K0 Ve	6.14	0.75	0.33		70.2	5.37
GJ 1002	00 04 13	-07 47.5	2.041	203.6	-42	M5-5.5	13.75	1.98	+1.60:	1.63	212.8	15.39
GJ 1003	00 04 46	+28 58.8	1.890	127.2		m	14.18	1.49	1.40	1.14	53.5	12.82

[11]

Figure 24: Part of a sample star catalog

Appendix B Calculation Results

B.1 The Twelve Results of The Navigation Star Selection Algorithm and Validation

- **Condition 1:** Bright and sparse

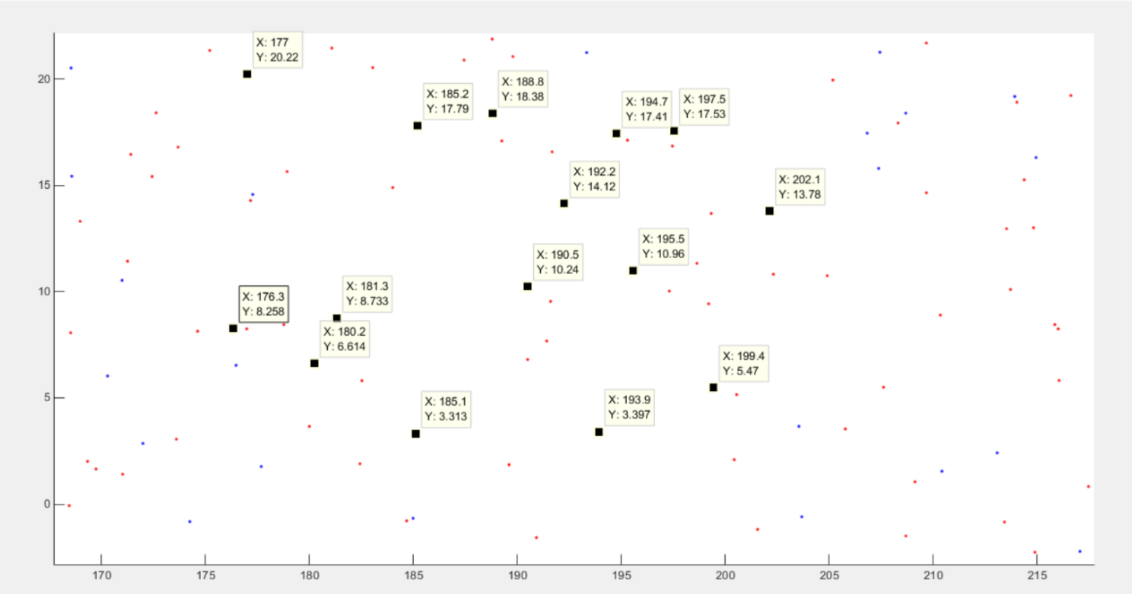

Figure 25: The plot of selected region, $\varepsilon = 5.4796$

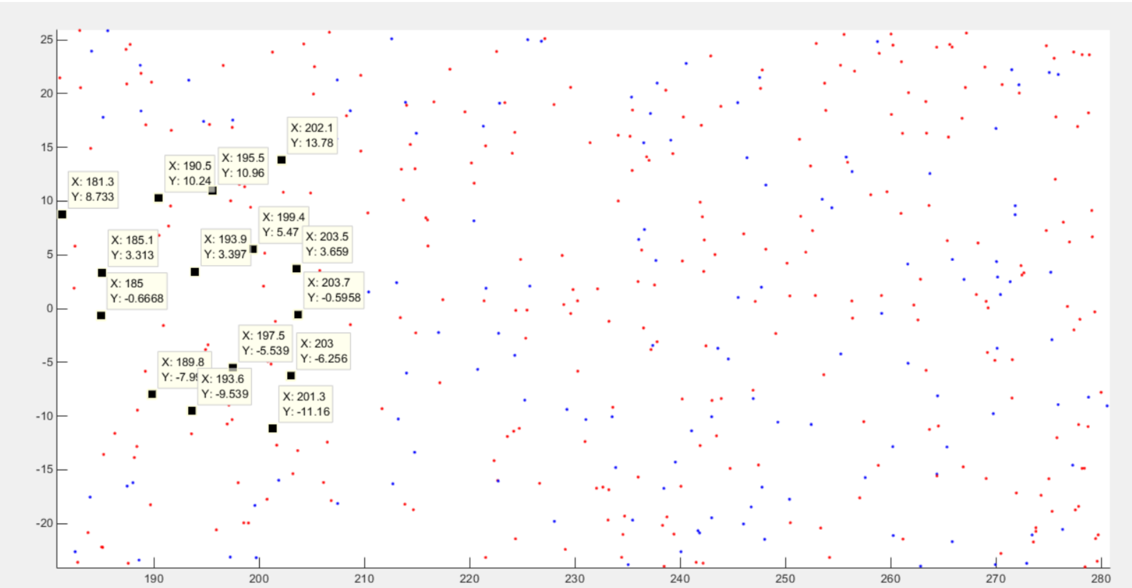

Figure 26: The plot of selected region, $\varepsilon = 12.0920$

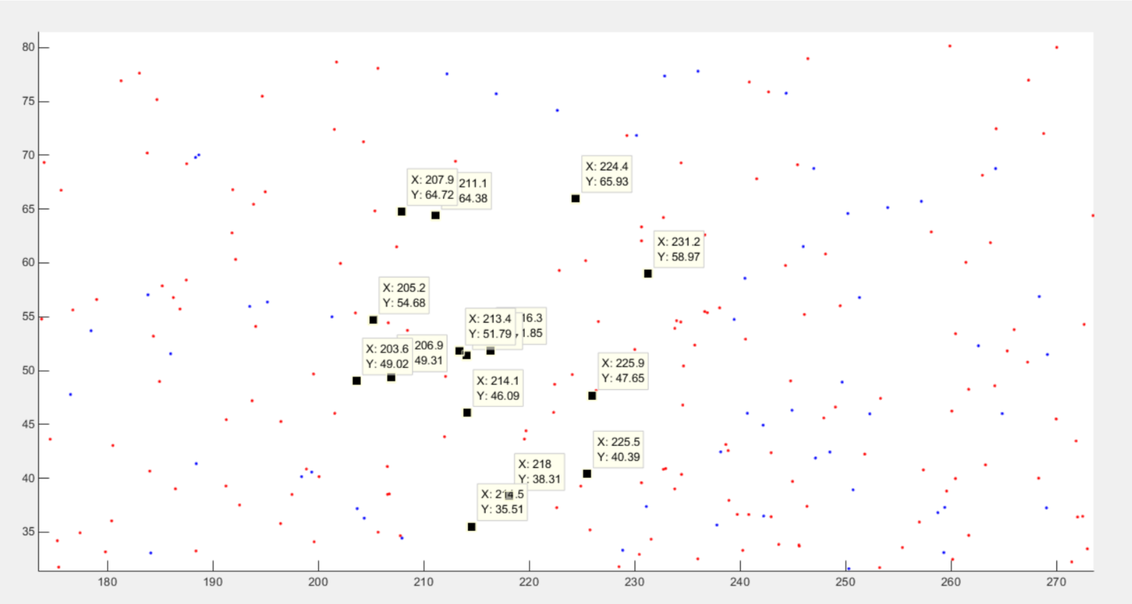

Figure 27: The plot of selected region, $\varepsilon = 12.9183$

- **Condition 2:** Bright and dense

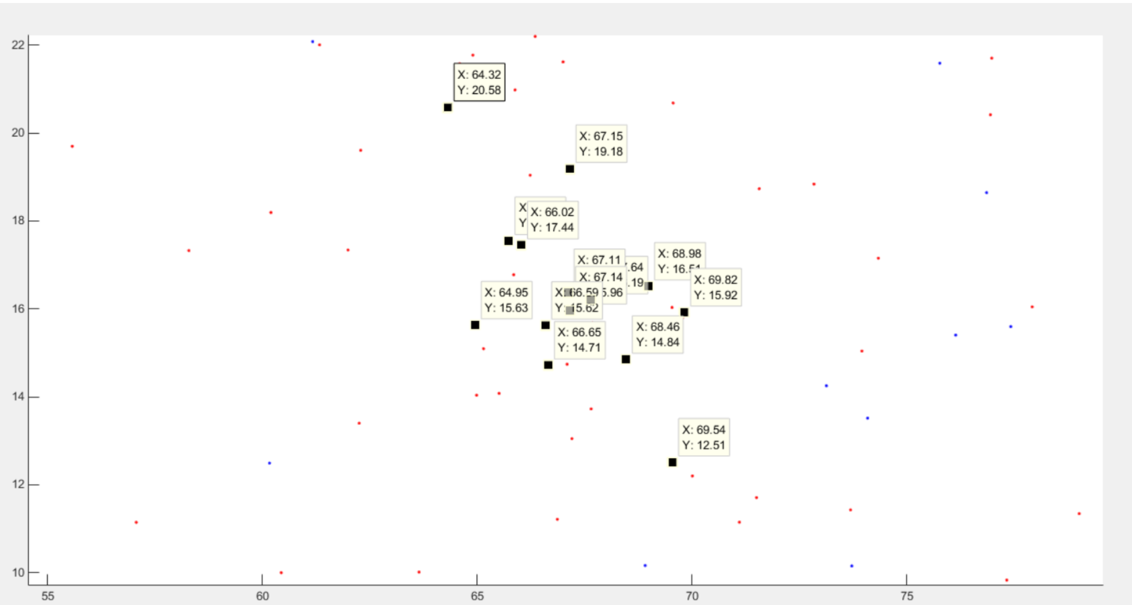

Figure 28: The plot of selected region, $\varepsilon = 2.9914$

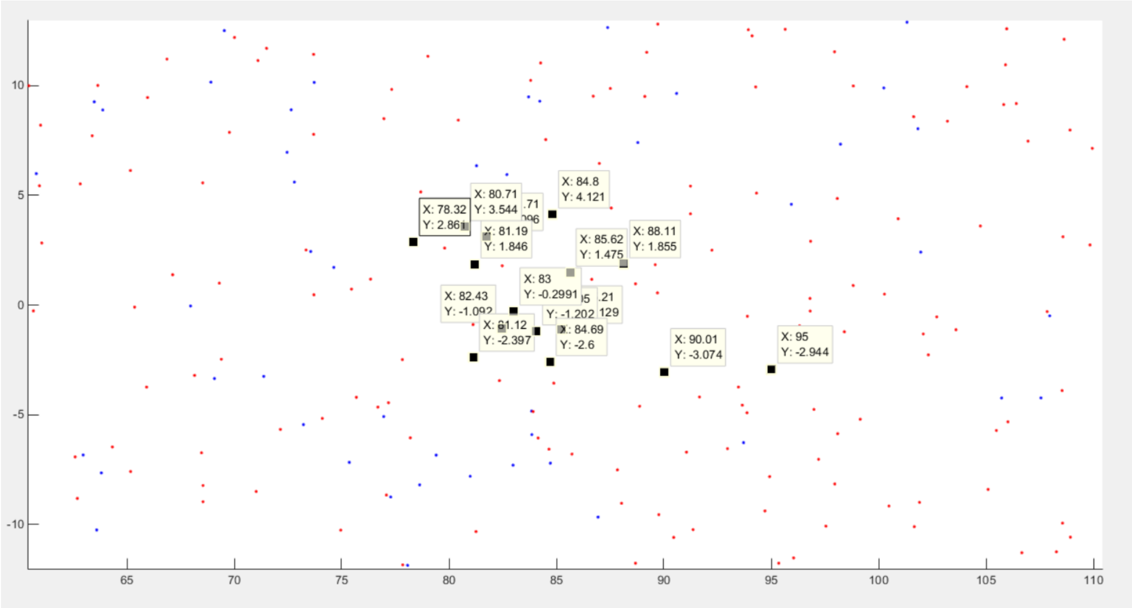

Figure 29: The plot of selected region, $\varepsilon = 8.9973$

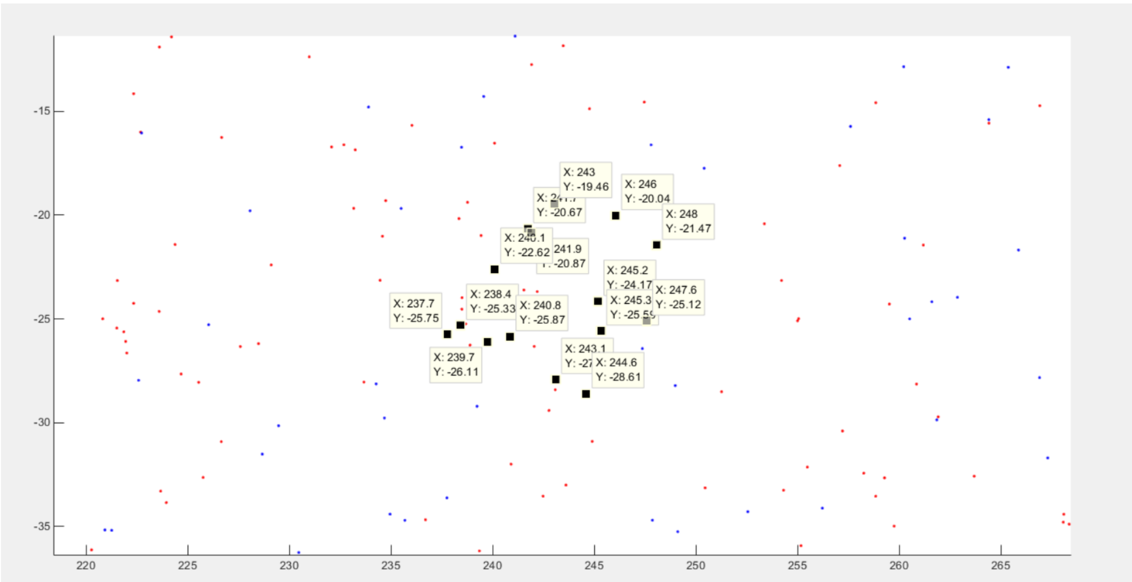

Figure 30: The plot of selected region, $\varepsilon = 0.1180$

- **Condition 3:** Dim and sparse

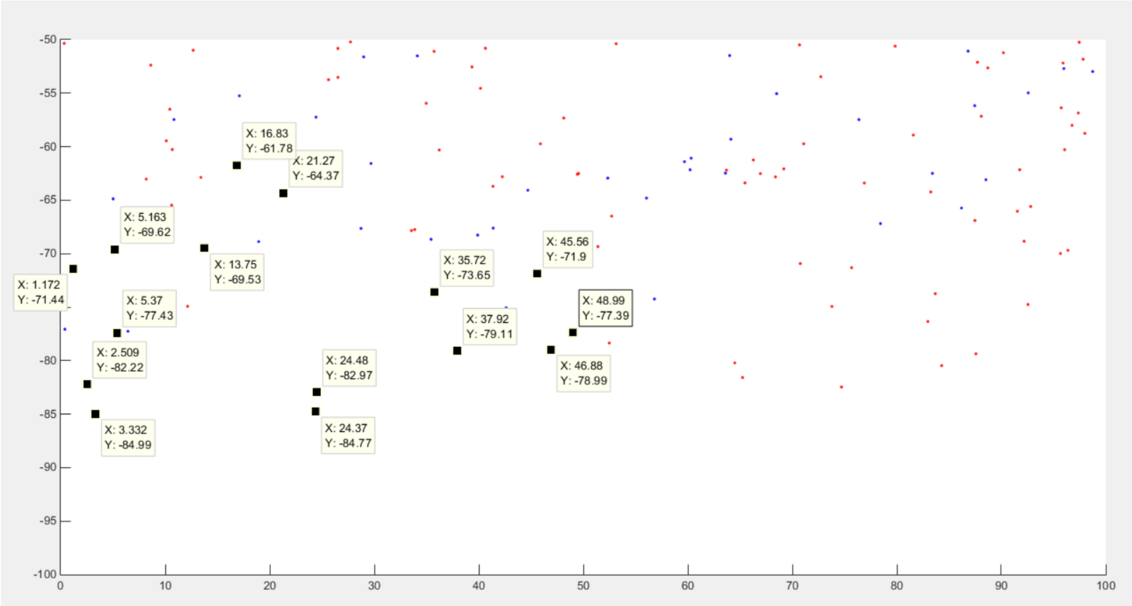

Figure 31: The plot of selected region, $\varepsilon = 3.4526$

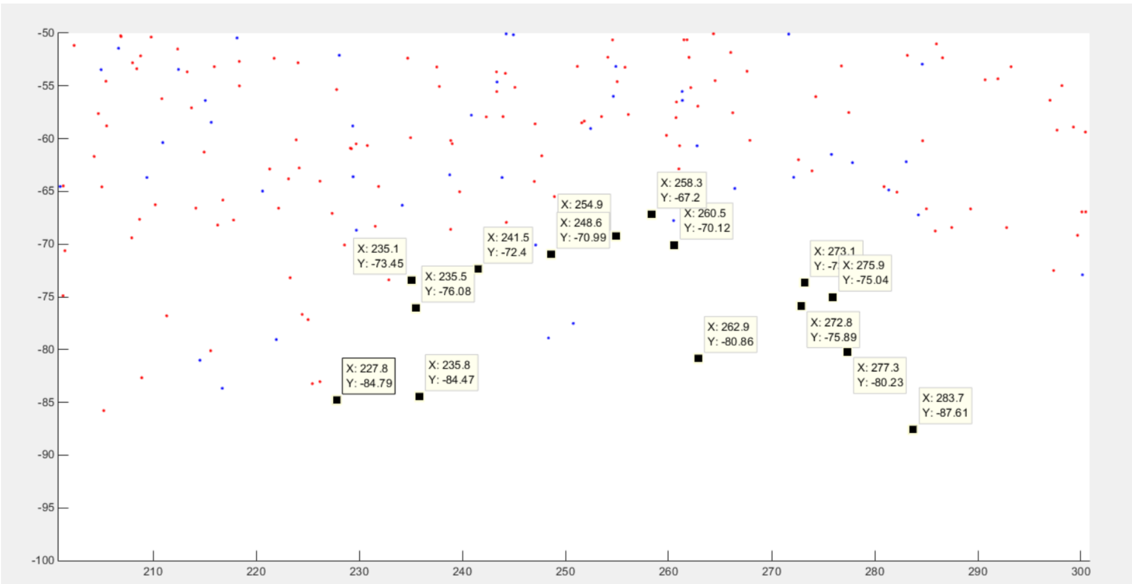

Figure 32: The plot of selected region, $\varepsilon = 13.6996$

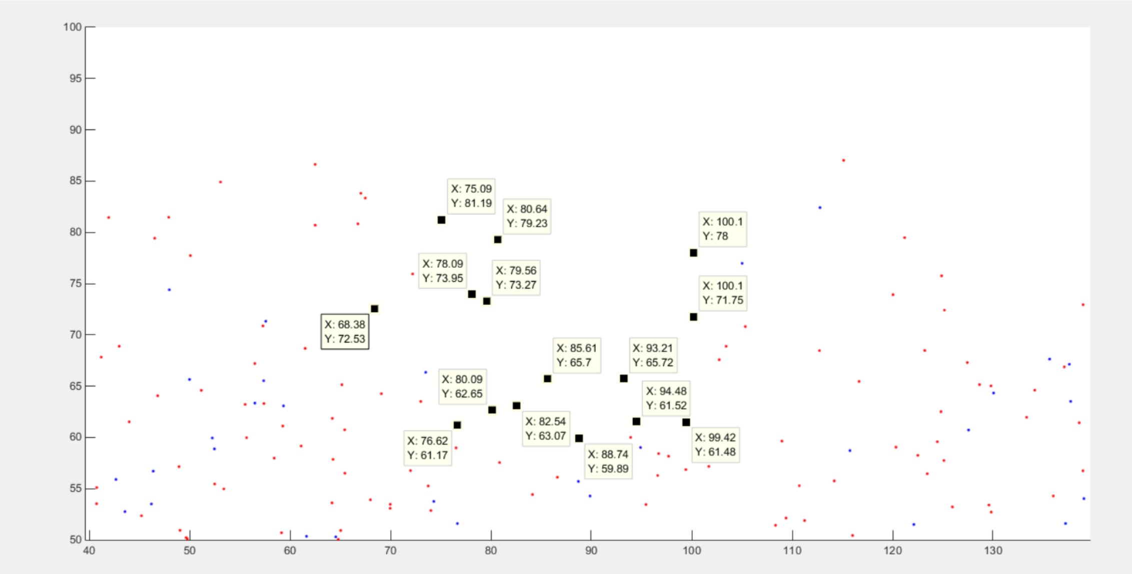

Figure 33: The plot of selected region, $\varepsilon = 11.5610$

- **Condition 4:** Dim and dense

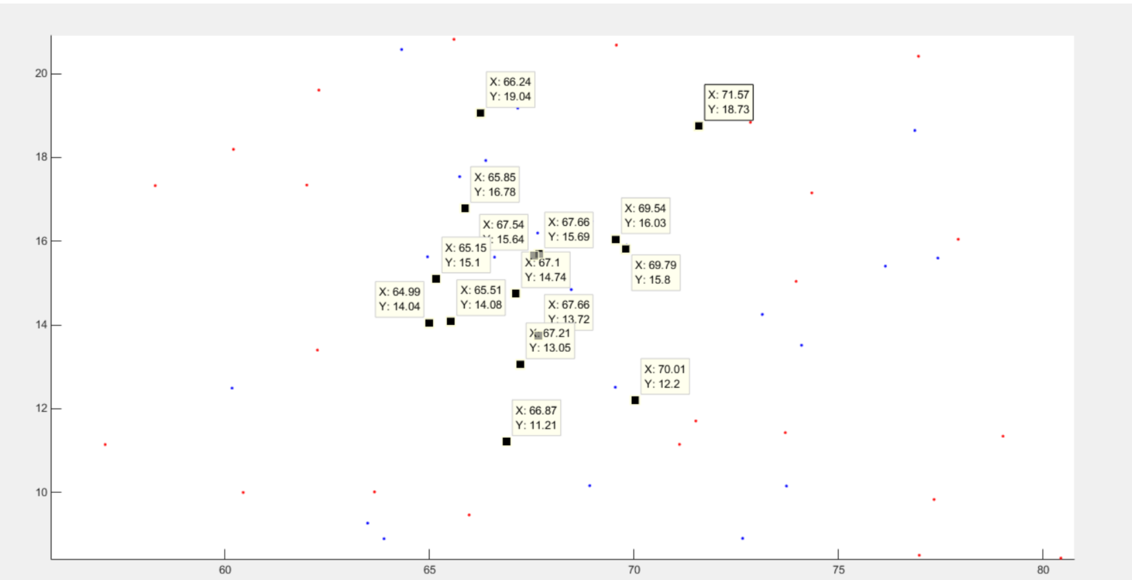

Figure 34: The plot of selected region, $\varepsilon = 10.8948$

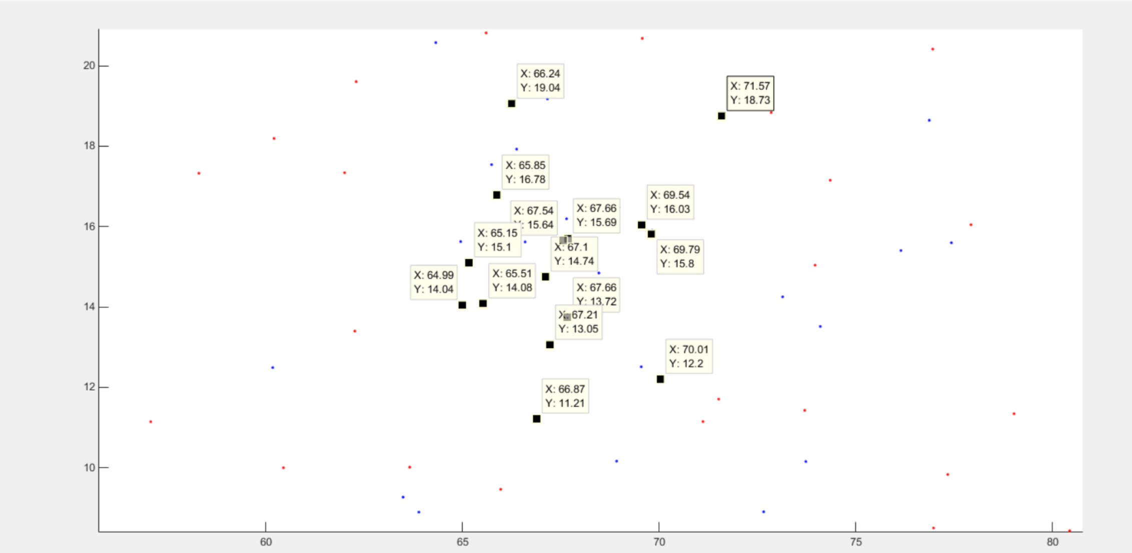

Figure 35: The plot of selected region, $\varepsilon = 7.0012$

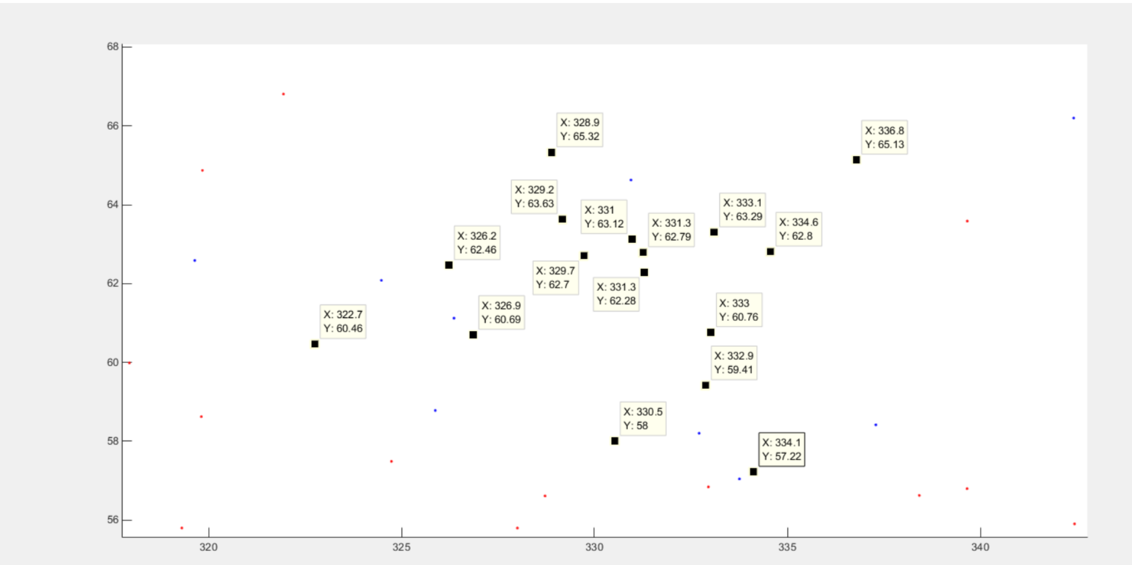

Figure 36: The plot of selected region, $\varepsilon = 7.0637$